Available online at www.sciencedirect.com
SCIENCE DIRECT®
Journal of Chromatography A, 1061 (2004) 159–165
JOURNAL OF CHROMATOGRAPHY A
www.elsevier.com/locate/chroma

Novel biporous polymeric stationary phase for high-speed protein chromatography

Guo-Yong Sun, Qing-Hong Shi, Yan Sun*

Department of Biochemical Engineering, School of Chemical Engineering and Technology, Tianjin University, Tianjin 300072, China

Received 24 May 2004; received in revised form 28 October 2004; accepted 28 October 2004

Abstract

A novel rigid biporous bead (BiPB) had been fabricated by double emulsification to prepare a (w/o)/w emulsion and a subsequent polymerization. The polymerization of monomers, glycidyl methacrylate and ethylene glycol dimethacrylate, was initiated with benzoin ethyl ether by ultraviolet irradiation. The BiPB with an average diameter of 42.8 μm was characterized to possess two types of pores, i.e., micropores (20–100 nm) and superpores (300–4000 nm). Its specific surface area was determined to be 41.9 m^2/g, about 20% smaller than that of a microporous bead (MiPB) (52.1 m^2/g). Flow hydrodynamic experiments showed that the BiPB column had smaller backpressure and plate height than those of the MiPB column at a given flow rate. Derivatized with diethylamine (DEA), the static adsorption capacity of the DEA-BiPB was about 7% smaller than that of the DEA-MiPB for BSA (bovine serum albumin). However, frontal analysis demonstrated that the dynamic binding capacity of the DEA-BiPB column was 1.6–2.4 times higher than that of the DEA-MiPB at high flow rate range of 1200–2400 cm/h. Moreover, separation of a model protein mixture (myoglobin and BSA) was conducted at mobile phase velocities up to 3000 cm/h to compare the performance of the two stationary phases. All the results indicate that the BiPB contains interconnected flowthrough pores and the BiPB column is promising for high-speed protein chromatography.

Keywords: Stationary phases, LC; Polymerization; Emulsification; Biporous medium; Proteins

1. Introduction

Liquid chromatography is one of the important tools for the purification of biological macromolecules because of its high resolution and mild separation conditions. In general, the target compounds present in dilute aqueous solution and the chemical nature of fermentation broth is quite complex, containing hundreds of contaminating species such as cell debris, nuclear acids, lipids, and protein species having similar physicochemical properties [1]. Meanwhile, the fragility of target protein is another challenge during the chromatographic separation. Long time exposure in artificial environment often leads to the loss of protein activity and fragmentation of the target. Therefore, it is of importance for protein purification protocols to curtail the chromatographic time in the maintenance of protein structure and its function [2].

The key element of LC is the stationary phase, and the progress of the stationary packings expands its application in bioseparations. At the beginning, polysaccharides, such as agarose, dextran and cellulose, were the most widely used chromatographic media for protein chromatography [3] because they were easily available and derivatizable, and of high porosity and high surface area. Nevertheless, their low mechanical strength constituted a limiting factor when using at high speed [4]. The use of inorganic supports, such as silica, could increase both the resolution and the operation speed

* Corresponding author. Tel.: +86 22 27404981; fax: +86 22 27406590.
E-mail address: ysun@tju.edu.cn (Y. Sun).

0021-9673/$ – see front matter © 2004 Elsevier B.V. All rights reserved.
doi:10.1016/j.chroma.2004.10.101

of chromatographic columns for the separation of proteins, but they often showed cation-exchange effects from residual silanol and limited stability at low or high pH, in particularly under basic conditions at pH > 9 [5,6]. Due to the polysaccharides and inorganic material's drawbacks, organic resins have been widely studied as alternatives. Organic resins usually present higher mechanical strength than soft gel and can tolerate extreme environmental conditions such as pH 1–12 [7].

However, relatively long time is required for the separation of biomolecules due to the slow diffusion of macromolecules through the interior of stationary phase. Thus, a new chromatography concept, called perfusion chromatography or flowthrough chromatography using packing materials with large through-pores or superpores, has been introduced to overcome the problem related to the interior mass transfer resistance [8]. The matrix for perfusion chromatography has primary and secondary sets of pores. This kind of perfusive (biporous) matrix can promote the intraparticle mass transfer by convective flow through the superpores [1,5,6,9]. Since the convective transport rate of biopolymer is several orders of magnitude greater than the diffusive rate, the interior binding sites within the pore network of a perfusive support are accessed more rapidly than the case with packing materials relying solely on diffusive transport. Accelerated mass transport resulting from intraparticle flow minimizes band broadening, which in turn is recognized as high column efficiency and high capture efficiency at elevated flow-rates [9–12].

The fabrication of commercial perfusion polymeric biporous resins involved preparing small particles using suspension, emulsion, or hybrid polymerization techniques and building up the particles into matrices of microns to tens of microns [1]. Moreover, it has been reported that superporous agarose beads could be prepared by a double emulsification procedure [13–15] and the superpore created by the interior oil phase could greatly improve the mass transfer. Inspired by their research, we have here introduced the double emulsification technique to fabricate rigid polymeric biporous medium using glycidyl methacrylate and ethylene glycol dimethacrylate as monomers by a radical suspension photo-polymerization by ultraviolet irradiation. The new biporous bead is expected to overcome the drawback of agarose gel in low mechanical strength and to take less time in preparation than those polymeric matrices reported previously [16–20]. Derivatized with diethylamine to create an anion exchanger, the matrix was used for ion-exchange protein chromatography. Its pore structure, pore size distribution and specific surface area were characterized and compared with those of a microporous matrix prepared by suspension-polymerization with organic solvents as porogen. The chromatographic properties, such as flow hydrodynamics, static and dynamic adsorption behavior, and column efficiency, were investigated. Protein separation was also performed to further confirm its usability in high-speed protein chromatography.

2. Materials and methods

2.1. Materials

Glycidyl methacrylate (GMA) with a purity of 99% was purchased from Suzhou Anli Chemical Company (Jiangsu, China) and used without further purification. Ethylene glycol dimethacrylate (EDMA), bovine serum albumin (BSA) and myoglobin were obtained from Sigma (St. Louis, MO, USA). Toluene and *n*-heptane were from Tianjin Chemical Company (Tianjin, China). Benzoin ethyl ether (BEE), a free radical initiator of photopolymerization, was purchased from the Medicine Co. Ltd. (Beijing, China). Sorbitan monooleate (Span 80) and polyoxyethyene sorbitanmonooleate (Tween 80) were obtained from Tianjin Kaitong Chemical Company (Tianjin, China). Diethylamine (DEA) was the product of Tianjin Kewei Chemical Company (Tianjin, China) and used without further purification. Other reagents were all of analytical grade from local sources.

2.2. Synthesis of polymeric beads

Biporous beads (BiPB) were prepared by a radical suspension photo-polymerization method. In a typical procedure, 5 ml of organic porogenic agent was prepared by mixing 3 ml toluene and 2 ml *n*-heptane. The organic porogen was added to a mixture of monomers (4.5 ml GMA and 3 ml EDMA) containing 0.08 g BEE and 0.45 g Span 80. The mixture was degassed and homogenized by ultrasonication for 20 min. Then the solution was transferred to a glass reactor and 8 ml of 20% glycerol solution was added. The two-phase system was rigorously stirred at 8000 rpm for 5 min to prepare water-in-oil (w/o) emulsion (emulsification I). The emulsion was then immediately poured into a reactor containing 60 ml aqueous solution of 4% Tween 80 at a stirring speed of 1600 rpm (emulsification II). After 1 min agitation at 1600 rpm, the (w/o)/w emulsion was transferred to a beaker (70 mm i.d.) agitated with magnetic stirrer at 300 rpm and irradiated with an ultraviolet lamp (1000 W) for 20 min for polymerization reaction. The white polymeric beads were collected and thoroughly washed with hot deionized water (60–70 °C). Then, the organic porogenic agent was removed by extracting the beads with ethanol under reflux for 24 h in a Soxhlet extraction apparatus. Finally, the beads were washed with deionized water thoroughly and dried at room temperature under vacuum (<130 Pa).

Microporous beads (MiPB) were prepared without the procedure of emulsification I described above. That is, the organic phase containing the organic porogen, monomers and initiator was directly added to the aqueous solution of 4% Tween 80 to prepare o/w emulsion. Other conditions and procedures were the same as those in the preparation of the BiPB.

2.3. Preparation of anion exchanger

Modification of the BiPB and MiPB with DEA was carried out as reported earlier [10]. Briefly, 5.0 g of drained

solid phase was added to the mixture of 25 ml dioxane and 25 ml DEA. Then, the slurry under stirring at 180 rpm was heated to 60 °C in thermostatted water bath and kept at that temperature for 6.5 h. After the coupling reaction, epoxide groups remaining on the polymer were reduced to hydroxyl groups at room temperature by suspending the solid phase in 100 ml of 0.1 mol/l $NaBH_4$ solution overnight in an incubator at a shaking speed of 180 rpm. The product was thoroughly washed with an excess of deionized water and ethanol in turn. The washing process was repeated 10–15 times over a week. Finally, the beads were dried at 50 °C for 24 h until the weight of beads became constant.

2.4. Characterization of the beads

Particle-size distribution of the beads was measured with a Mastersizer 2000 U (Malvern Instruments, UK). The pore structure of the adsorbents in dry state was observed by scanning electron microscopy (SEM) (S-3500N, Hitachi, Japan). All samples were sputter-coated with gold before analysis. The pore size distribution was determined by mercury porosimetry using a Quantanchrome Poremaster-60 mercury porosimeter (Quantanchrome Corporation, USA). The specific surface area of the dry particles was calculated from the BET isotherm of nitrogen, measured with a BET Chembet-3000 instrument (Quantanchrome Corporation, USA). Hydrated density of wet beads was measured with a 25 ml pycnometer.

The total ion capacity of the anion exchanger was detected by the following method. The beads (1.5 g) were suspended in 100 ml of 1 mol/l HCl solution in an incubator of 160 rpm at 25 °C for 12 h. After being drained by a G3 sinter glass filter, the beads were washed with an excess of ethanol until neutral washing ethanol was obtained. Then, the beads were suspended in 100 ml 0.5 mol/l sodium sulfate in an incubator of 200 rpm at 25 °C for 12 h. After being drained again by a G3 sinter glass filter, the Cl^- ions in the filtrate were titrated by 0.01 mol/l $AgNO_3$ solution. The same volume of fresh Na_2SO_4 solution was used as control. The total ion capacity was calculated by mass balance.

2.5. Static adsorption experiment

The finite batch adsorption experiment was utilized to determine the static adsorption isotherms of bovine serum albumin (BSA) on the DEA-BiPB and DEA-MiPB. At first, the beads were equilibrated with 10 mmol/l Tris–HCl buffer (pH 7.6). After being drained by a G3 sinter glass filter, the equilibrated ion exchanger (0.4 g) was transferred to a 25 ml Erlenmeyer flask containing 10 ml BSA solution with a protein concentration up to 2 mg/ml. Adsorption was performed at 25 °C in an incubator at a shaking speed of 160 rpm for 24 h. The protein concentration in supernatant was determined at 280 nm by Lamda 35 UV–vis spectrophotometer (Perkin-Elmer Instruments, USA). The bound amount of BSA was calculated by mass balance [16].

$$q = \frac{(c_0 - c)V\rho_w}{W} \quad (1)$$

where c_0 (mg/ml) and V (ml) are initial BSA concentration and protein solution volume, respectively; c and q (mg/ml wet resin) are respectively the liquid and solid phase BSA concentrations in equilibrium; W (g) and ρ_w (g/ml) stand for the mass and density of wet particles, respectively.

2.6. Chromatography

All the chromatography experiments were conducted on the ÄKTA Explorer 100 system controlled by Unicorn 4.11 software (Amersham Biosciences, UK) with an HR 5/10 column at room temperature. The column efficiency at flow velocities from 300 to 3000 cm/h was determined under a non-retained condition. The mobile phase was 0.3 mol/l NaCl in 10 mmol/l Tris–HCl buffer (pH 7.6). After equilibrating the column, 100 μl of BSA solution was injected, and the column was developed with the mobile phase and chromatogram was recorded at the column exit. The dead volume of the system was measured by injecting 100 μl of 20% acetone solution via the injection loop. The column efficiency was expressed as the height equivalent to a theoretical plate (HETP), which was determined by the moment analysis method [10].

Frontal analysis experiments were conducted in 10 mmol/l Tris–HCl buffer (pH 7.6) to determine the dynamic binding capacity. The protein solution was prepared by dissolving BSA into the mobile phase at 2.0 mg/ml. After equilibrating the column with 10 column volumes (CVs) of the mobile phase, protein solution was loaded into the column by a 50 ml Superloop (Amersham Biosciences, Sweden) and the protein concentration at the outlet was measured with a UV monitor. The breakthrough profile at the outlet was recorded until the absorbance of the outlet stream reached a platform. Finally, the column was cleaned by 5 CVs of 1.0 mol/l NaCl in the Tris–HCl buffer. The dynamic capacity at 10% breakthrough was calculated from Eq. (2) [11].

$$q_{10} = \frac{c_f F(t_{10} - t_0)}{V_B} \quad (2)$$

where q_{10} (mg/ml wet resin) is the dynamic binding capacity at 10% breakthrough, c_f (mg/ml) is the feed BSA concentration, t_{10} (min) is the time at 10% breakthrough, t_0 (min) is the retention time under non-retained condition, F (ml/min) is the volumetric flow rate and V_B (ml) is the bed volume.

2.7. Protein separation

A mixed solution of myoglobin and BSA was separated on the DEA-BiPB and DEA-MiPB columns at elevated flow rates to compare their performances in high-speed chromatography. After equilibrating the column with 10 mmol/l Tris–HCl buffer, pH 7.6 (buffer A), 100 μl of sample solution containing 0.5 mg/ml myoglobin and 1 mg/ml BSA was

injected and the column was washed with 2 ml of buffer A. Then, linear gradient elution was carried out by a change from buffer A to buffer B (1.0 mol/l NaCl in buffer A) in 5 CVs (10 ml). Protein concentration was detected at 280 nm. After each run, the column was cleaned with 10 CVs of buffer B. The column equilibration was performed with buffer A until a constant UV baseline was obtained.

3. Results and discussion

3.1. Physical properties of the beads

Fig. 1 shows SEM photographs of the BiPB and MiPB. Compared to the smooth surface of MiPB in Fig. 1c, the rough surface of the BiPB in Fig. 1a implies that there is significant difference on pore construct between these two types of beads. It is attributed to the presence of the superpores created by the micro-droplets of glycerol solution inside the polymeric beads. At a larger magnification, highly reticular, three-dimensional porous structure of the BiPB is particularly evident (Fig. 1b) as compared to the MiPB (Fig. 1d). Wide channels with pore sizes larger than 1 μm distribute on the surface of the BiPB, and some of them are expected to provide an interconnected path for convective flow in chromatography.

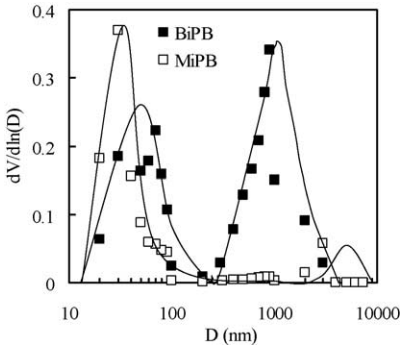

Fig. 2. Pore size (D) distributions of BiPB and MiPB.

The pore size distributions of the BiPB and MiPB were analyzed by mercury porosimetry (Fig. 2). It is clearly seen from Fig. 2 that there is a bimodal pore size distribution in the BiPB. The micropores mostly range from 20 to 100 nm, which are expected to act as the diffusive pores for solute transport. In comparison, the superpores distributes between

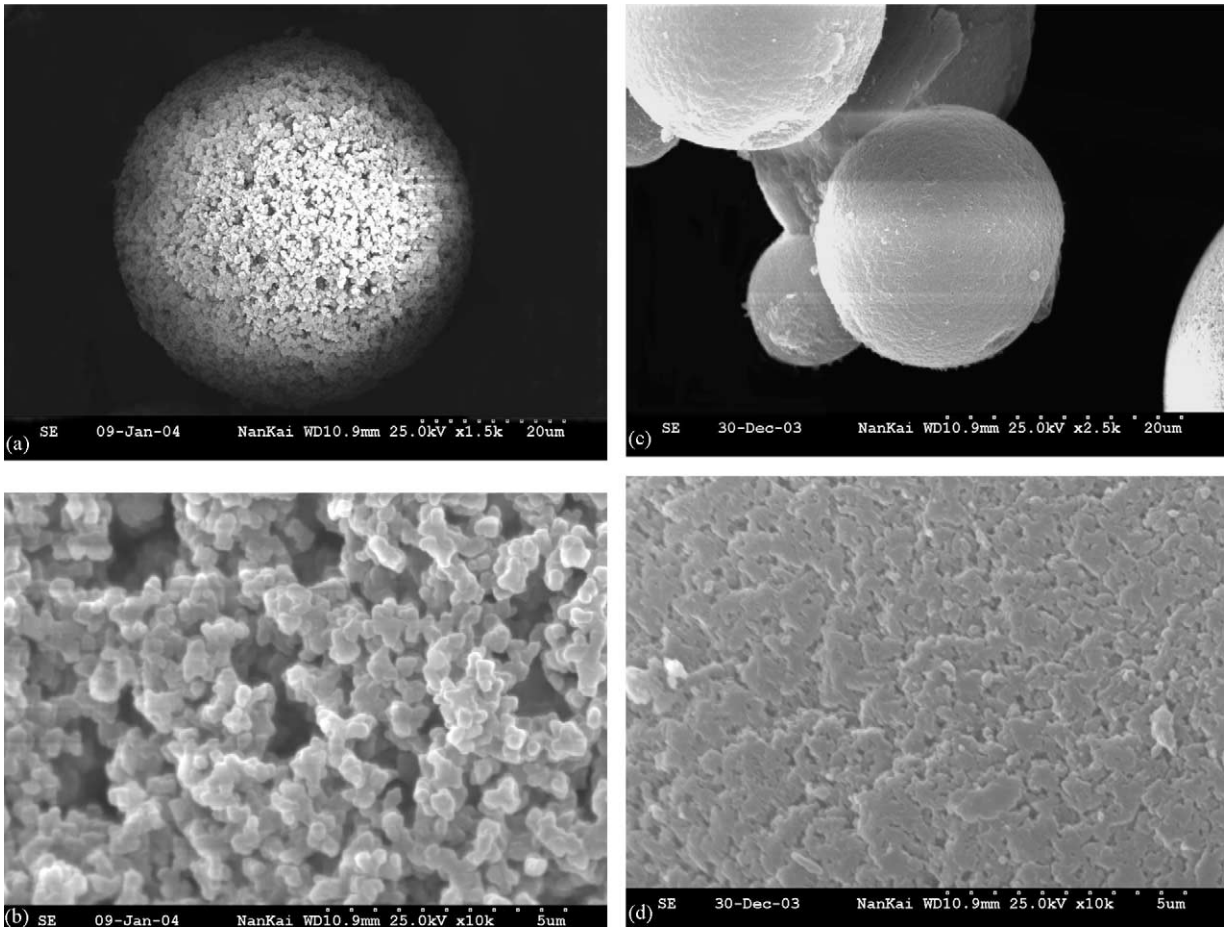

Fig. 1. SEM photographs of BiPB at a magnification of (a) ×1500 and (b) ×10,000 and of MiPB at a magnification of (c) ×1500 and (d) ×10,000.

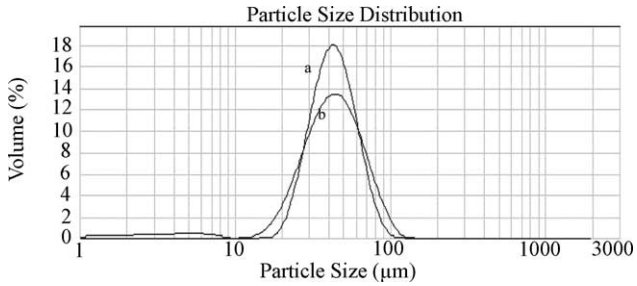

Fig. 3. The size distribution of (a) BiPB and (b) MiPB.

300 and 4000 nm, mostly larger than 600 nm. If the superpores are interconnected, convective flow through them can certainly occur during a chromatographic operation [1,5,6]. This will be further discussed below in protein chromatography.

In comparison to the BiPB, most pores in the MiPB are in the range of 20–100 nm, and only a small amount of micron-sized pores are identified. The small amount of wide pores might be those between small particles, which were regarded as pores by mercury porosimetry. Therefore, it is considered the MiPB contains mainly micropores through which solutes can transport by diffusion [11].

Specific surface area of an adsorbent is one of the indicators of its binding capacity, and a high specific surface area is often an essential necessity for the stationary phase of chromatography. The BET method revealed that the specific surface areas of the BiPB and MiPB were 41.9 and 52.1 m^2/g, respectively. The smaller specific surface area of the BiPB, compared to that of the MiPB, may be attributed to the existence of the superporous in the BiPB, which contributed less to the specific surface area than the micropores.

The hydrated densities of the BiPB and MiPB were estimated at 1.08 and 1.11 g/ml, respectively. The size distributions of both the adsorbents are shown in Fig. 3. The volume weighted mean diameters of the beads are almost the same, 42.8 μm for the BiPB and 42.4 μm for the MiPB. The total ion capacities of BiPB and MiPB were determined to be 0.172 and 0.213 μmol Cl^-/ml wet resin, respectively.

3.2. Flow hydrodynamics

Fig. 4 shows the effect of flow velocity on the backpressures of the BiPB and MiPB columns. It can be seen that the backpressure of the BiPB column was much lower and it increased almost linearly with the flow velocity up to 3600 cm/h. In contrast, the backpressure curve for the MiPB column was somewhat upward concave. It might be partly due to the presence of fine particles (1–8 μm) in the MiPB bulk (Fig. 3), which made the MiPB column more compact than that of the BiPB. However, the low backpressure of the BiPB column may be an evidence for the presence of the flow-through channels which reduced the flow resistance. The same phenomenon has been reported with other biporous

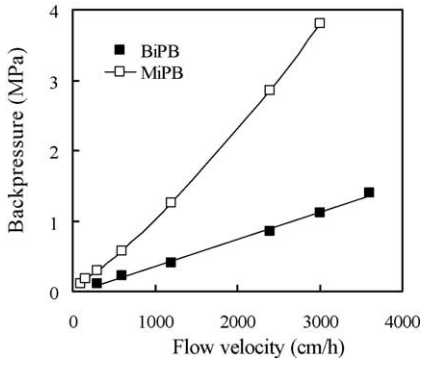

Fig. 4. Effect of flow velocity on backpressure of the BiPB and MiPB columns. Column: HR 5/10 (5 mm i.d., 10 cm length, 1.96 ml beads). Mobile phase: 10 mmol/l Tris–HCl buffer, pH 7.6.

beads [10–12]. Thus, the BiPB column enables an operation at high flow rate.

3.3. Column efficiency

The height equivalent to theoretical plate (HETP) was defined to describe the overall column efficiency and measured for a protein solute (BSA) under the unretained condition. Fig. 5 illustrates the relationship between HETP and flow velocity for both the BiPB and MiPB columns. At the lowest velocity tested (300 cm/h), the HETP of DEA-MiPB column (2.06 mm) was about 2.5 times larger than that of the DEA-BiPB column (0.82 mm). With increasing the flow velocity, the difference between the HETP values of the DEA-BiPB and DEA-MiPB columns was further augmented. That is, the HETP of the DEA-BiPB column appeared to increase slightly with flow rate up to 3000 cm/h, while that of the MiPB column showed a significant dependency on the flow velocity. This is a further evidence of the presence of the flow-through pores in the BiPB. With an increase of mobile phase velocity, more superpores in the BiPB are expected to be involved in the convective mass transport and the increase of HETP with increasing flow rate due to diffusion resistance can be greatly alleviated [6].

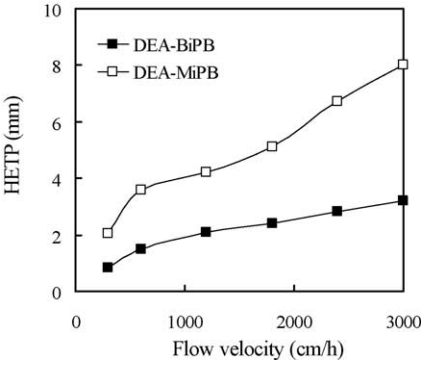

Fig. 5. Column efficiency detected with BSA as a function of mobile phase flow rate. Column: HR 5/10. Sample: 100 μl of 2 mg/ml BSA solution. Mobile phase: 0.3 mol/l NaCl in10 mmol/l Tris–HCl buffer, pH 7.6.

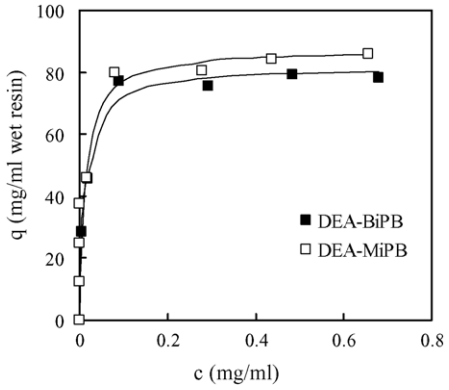

Fig. 6. Static adsorption isotherms of BSA to the DEA-BiPB and DEA-MiPB.

3.4. Static and dynamic adsorption

The static adsorption of BSA was investigated by finite batch adsorption to provide adsorption isotherms of the adsorbents. Fig. 6 shows the results. It is found that the Langmuir formulism can be applied to fit the experimental data:

$$q = \frac{q_m c}{K_d + c} \quad (3)$$

where c (mg/ml) is the equilibrium concentration in bulk solution, q (mg/g wet bead) is the adsorbed density of protein, q_m (mg/g wet bead) is the adsorption capacity, and K_d (mg/ml) is the dissociation constant. The static BSA adsorption capacities thus estimated from Eq. (3) were 81.7 mg/ml wet bead for the DEA-BiPB and 87.3 mg/ml wet bead for the DEA-MiPB. The static capacity of the DEA-BiPB was only 7% smaller than that of the DEA-MiPB, indicating that the presence of the superpores in the BiPB did not significantly reduce the q_m.

It is more significant for an adsorbent to show rather high dynamic or chromatographic capacity than high static capacity. Frontal analysis by breakthrough experiments can provide with the dynamic binding capacity (DBC). The DBC values of the DEA-BiPB and DEA-MiPB columns, calculated from Eq. (2), as a function of flow velocity are given in Fig. 7.

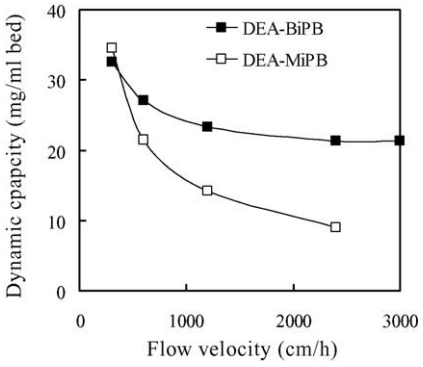

Fig. 7. Dynamic binding capacities of BSA on the DEA-BiPB and DEA-MiPB columns.

At the lowest flow rate tested (300 cm/h), the DBC of the DEA-MiPB column (34.5 mg BSA/ml bed) was even somewhat higher than that of the DEA-BiPB column (32.6 mg BSA/ml bed). With increasing the mobile phase velocity, however, the DBC of the MiPB column decreased drastically to a value of 8.9 mg/ml bed at 2400 cm/h. In contrast, the DBC of the DEA-BiPB column decreased slowly and kept a value of 21.3 mg/ml bed up to a flow rate of 3000 cm/h. In other words, in the high flow rate range of 1200–2400 cm/h, the DBC of the DEA-BiPB column was 1.6–2.4 times higher than that of the DEA-MiPB column. The results indicate that the onset of the convective flow within the superpores accelerated the intraparticle mass transfer [8], leading to the high column efficiency (Fig. 5) and dynamic binding capacity at elevated flow velocity.

After the frontal analysis experiments, the adsorbed protein was recovered by elution with 1.0 mol/l NaCl in Tris–HCl

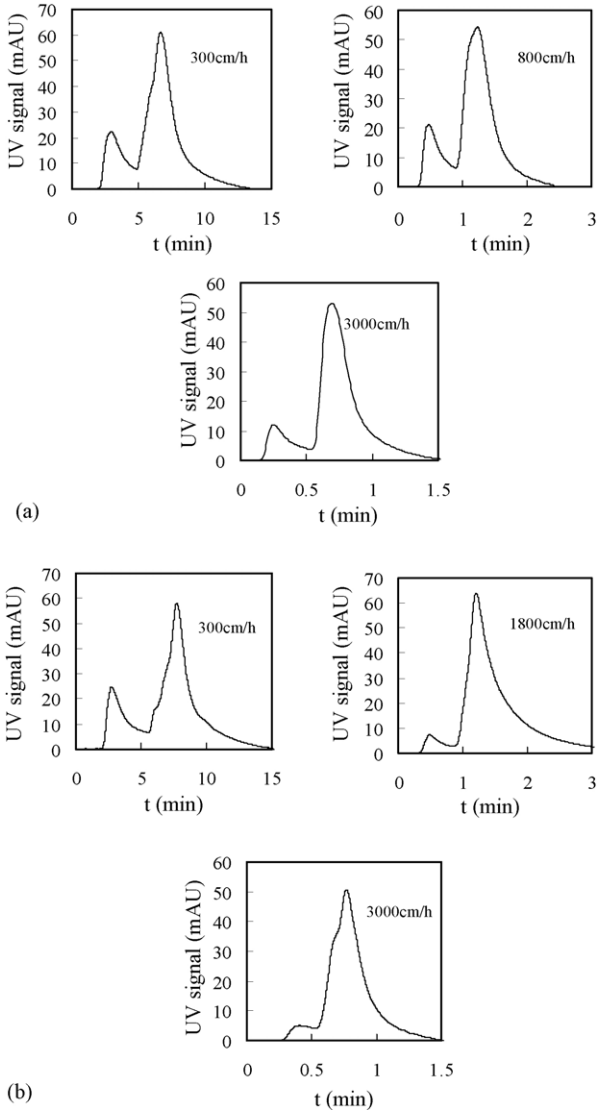

Fig. 8. Separation of (1) myoglobin and (2) BSA on (a) DEA-BiPB and (b) DEA-MiPB columns at different flow rates.

buffer (pH 7.6). As a result, the adsorbed BSA was found completely eluted by the high ionic strength solution, indicating the absence of nonspecific adsorption of the matrices for the protein.

3.5. Protein separation

To further demonstrate the advantage of the BiPB column in high-speed protein chromatography, a mixture of model proteins, myoglobin and BSA, was separated at different flow rates (Fig. 8). With the BiPB column, the shape of the protein chromatograms and resolution of the proteins were less affected by mobile phase velocity up to 3000 cm/h. With the MiPB column, however, the resolution decreased significantly with increasing the flow rate. At the flow rate higher than 1800 cm/h, most myoglobin was mixed to the BSA peak. The results further demonstrate that the BiPB column is promising for high-speed protein chromatography.

All the results described above have indicated that the MiPB column had poorer performance than the BiPB column. As shown in Fig. 2, the average pore size of the MiPB was about 30 nm. This value is comparable to the average pore diameter of Sepharose CL-6B (35 nm) [21], which is a widely used medium for protein chromatography. In addition, the pore size of the MiPB was in the range of 10–100 nm, similar to most protein adsorbents. Thus, the poor performance of the MiPB column is likely due to the poor pore structure rather than the pore size. Consequently, the introduction of convective pores greatly improved the intraparticle mass transport. It leads to higher column efficiency (Fig. 5), dynamic capacity (Fig. 7) and protein resolution (Fig. 8) of the BiPB column than those of the MiPB column, especially at high flow rates.

4. Conclusions

Using glycerol solution and *n*-heptane/toluene organic solvent as porogenic agents to respectively create superpores and micropores, a novel biporous matrix has been prepared by double emulsification and UV-irradiated polymerization. The biporous structure of the medium was identified by SEM observations and pore size analysis. Convective flow of mobile phase through the superpores in the biporous medium has also been confirmed by its low column backpressure, high column efficiency, high dynamic binding capacity and high protein resolution at high flow rate. All the results indicate that the biporous adsorbent is promising for high-speed protein chromatography. It is considered that optimization of the fabrication procedure would enable to further improve the performance of the biporous stationary phase.

Acknowledgment

This work was supported by the National Natural Science Foundation of China (Nos. 20025617 and 20276051).

References

[1] N.B. Afeyan, F.E. Regnier, R.C. Dean, U.S. Patent No. 5,019,270, 1991.
[2] E. McCarthy, G. Vella, R. Mhatre, Y. Lim, J. Chromatogr. A 743 (1996) 163.
[3] J. Porath, P. Flodin, Nature 183 (1959) 1657.
[4] L.E. Weaver Jr., G. Carta, Biotechnol. Progr. 12 (1996) 342.
[5] N.B. Afeyan, S.P. Fulton, F.E. Regnier, J. Chromatogr. 544 (1991) 267.
[6] N.B. Afeyan, N.F. Gordon, L. Mazasaroff, L. Varady, S.P. Fulton, Y.B. Yang, F.E. Regnier, J. Chromatogr. 519 (1990) 1.
[7] M.C. García, M.L. Marina, M. Torre, J. Chromatogr. A 880 (2000) 169.
[8] F.E. Regnier, Nature 350 (1991) 634.
[9] A.E. Rodrigues, Z.P. Lu, J.M. Loureriro, Chem. Eng. Sci. 46 (1991) 2765.
[10] Y. Shi, Y. Sun, Chromatographia 57 (2003) 29.
[11] Y. Shi, X.Y. Dong, Y. Sun, Chromatographia 55 (2002) 405.
[12] L. Wu, S. Bai, Y. Sun, Biotechnol. Prog. 19 (2003) 1300.
[13] P.-E. Gustavsson, P.-O. Larsson, J. Chromatogr. A 734 (1996) 231.
[14] P.-E. Gustavsson, K. Mosbach, K. Nilsson, P.-O. Larsson, J. Chromatogr. A 776 (1997) 197.
[15] P.-O. Larsson, U.S. Patent No. 5,723,601, 1998.
[16] M.L. Zhang, Y. Sun, J. Chromatogr. A 922 (2001) 77.
[17] Y.H. Yu, Y. Sun, J. Chromatogr. A 855 (1999) 129.
[18] Q.Z. Luo, H.F. Zou, Q. Zhang, X.Z. Xiao, J.Y. Ni, Biotechnol. Bioeng. 80 (2002) 481.
[19] E.J. Boschetti, J. Chromatogr. A 658 (1994) 207.
[20] X. Zhou, B. Xue, S. Bai, Y. Sun, Biochem. Eng. J. 11 (2002) 13.
[21] J.C. Bosma, J.A. Wesselingh, AIChE J. 44 (1998) 2399.